COMMISSIONS G1 AND G4 OF THE IAU
INFORMATION BULLETIN ON VARIABLE STARS
Volume 63 Number 6240 DOI: 10.22444/IBVS.6240

Konkoly Observatory
Budapest
05 April 2018

HU ISSN 0374 – 0676

2MASS J06422218-0226285 - A NEW OUTBURST SOURCE†

BLEX, SUSANNE[1]; HACKSTEIN, MORITZ[1]; HAAS, MARTIN[1]; KIMESWENGER, STEFAN[2,3]; CHINI, ROLF[1,2]; HODAPP, KLAUS[4]

[1] Astronomisches Institut, Ruhr-Universität Bochum, Germany; e-mail: sublex@astro.rub.de

[2] Instituto de Astronomía, Universidad Católica del Norte, Chile

[3] Institute for Astro- and Particle Physics, University of Innsbruck, Austria

[4] Institute for Astronomy, University of Hawaii, USA

Abstract

We discovered the outburst of 2MASS J06422218–0226285. Between end 2012 and early 2014, this object brightened by 3 mag in r and i, and by 3.7 mag in J. Since then, it has stayed at high brightness of about 16 mag in r and 15 mag in i. Possible explanations for this kind of light curve might be a Catalysmic Variable, a Symbiotic Binary or a FUor or EXor type Young Stellar Object. The color properties favor an outbursting Young Stellar Object.

2MASS J06422218–0226285 brightened between the end of 2012 and early 2014 by about 3 mag in r and i, and by 3.7 mag in J, and has stayed at high brightness since then.

This object has been photometrically surveyed by several missions at optical and infrared wavelengths. Among these surveys are GSC II in 1991 (Lasker et al. 2008), 2MASS in 1998 (Skrutskie et al. 2006), DENIS in 2000 (Epchtein et al. 1994), IPHAS in 2006 (Barentsen et al. 2014), and WISE in 2010 (Wright et al. 2010). Viironen et al. (2009) described J06422218–0226285 as a planetary nebula (PN) and also have found that Hα probably has been in emission before the outburst. There is no prominent star forming region close to the object.

While analyzing exceedingly red and variable objects among the Galactic Disc Survey (GDS, Haas et al. 2012, Hackstein et al. 2015), Blex (2017) discovered the brightening of 2MASS J06422218–0226285 (or GDS J064221-022628). The discovery of the outburst motivated further measurements at the Universitätssternwarte Bochum (USB) near Cerro Armazones, Chile. Between November 23$^{\rm rd}$ and December 12$^{\rm th}$ in 2017, the latest optical data in the B, V, r, and i filters have been collected. During three nights in February to March 2018, we were able to obtain narrow-band spectro-photometry of HeI, H_2 (1-0) S1, Brγ, CO, and K_c, as wll as JHK_s broadband photometry. Our search for Hα emission after the outburst using narrow bands at 6450, 6563 and 6721 Å has failed due to a too low object brightness and poor S/N at these wavelengths.

Figure 1 shows the r- and i-band light curves from the GDS together with previous photometry of GSC II, DENIS, and IPHAS (Barentsen et al. 2014) data points. The light

†Based on data collected under the ESO/RUB — USB agreement at the Paranal Observatory

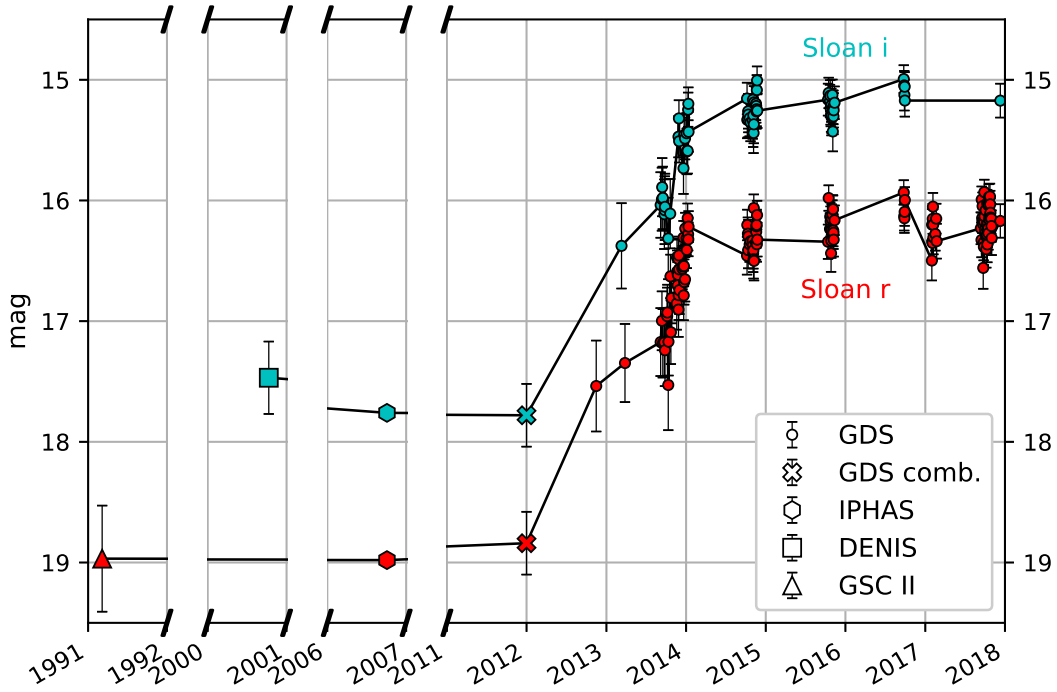

Figure 1. GDS light curve in r and i with additional IPHAS, DENIS, and GSC II data points; the IPHAS error is smaller than the symbol size.

curve values are listed in Tables 2 and 3 (at the end of the paper). The latest measurement in December 2017 yielded an r magnitude of 16.170 ± 0.139 and an i magnitude of 15.173 ± 0.140. A check of the single segments of the GDS light curve showed no short-term periodicity. The GSC II, IPHAS, and GDS measurements suggest a constant brightness of about $r = 19$ mag between 1991 and 2012. A constant faint state lasting back from 1991 to 1955 is further supported by the sequence of past DSS1, DSS2, and present GDS image cutouts (Fig. 2).

The optical to mid-infrared spectral energy distribution (SED) is depicted in Fig. 3, separated for both faint and bright states. Already before 2012, J06422218–0226285 has shown an infrared excess in the 2MASS and WISE color-color diagrams, consistent with a classical T Tauri star surrounded by circumstellar dust. After the outburst, the star has become much redder, suggesting dispersed dust. Although Hα does not appear in emission after the outburst, a strong P Cygni-type absorption could balance out potential emission.

Our near-infrared JHK_s and narrow-band spectro-photometry reveals a potential Brackett–gamma (Brγ) emission (Fig. 4, Tab. 1). The resulting Brγ flux would be about $5.1 \cdot 10^{-17}$ W/m^2, comparable to the range found by Carr et al. (1990) for Young Stellar Objects (YSOs). The large Brγ equivalent width of about 19 Å would place J06422218–0226285 among strongly accreting YSOs. In this scenario, the increase in brightness can be explained as a FUor- or EXor-type outburst.

Furthermore, matching with 2MASS allowed for searching the environment of J06422218–0226285 for K-excess objects in the JHK_s color-color diagram, which lie at least 2σ right-hand of the slope $(J - H) = 1.7\,(H - K) - 0.12$. We considered only

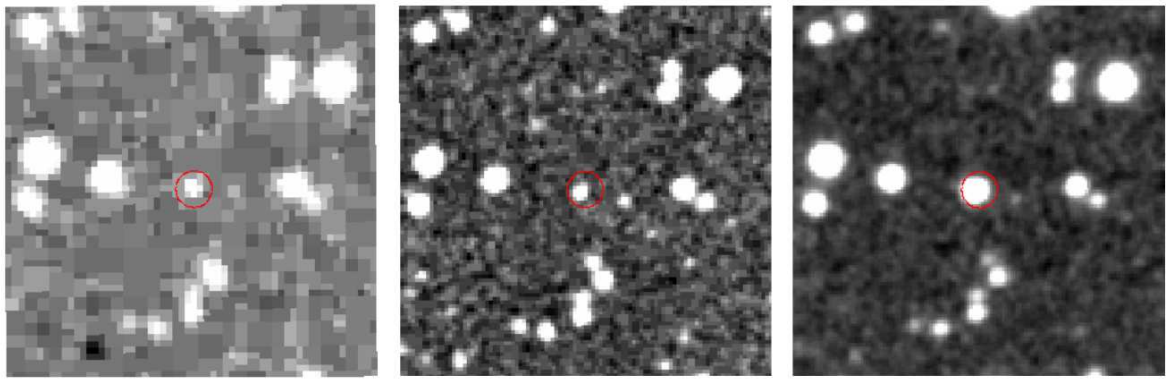

(a) *DSS1 1955* **(b)** *DSS2 1991* **(c)** *GDS 2012-2017*

Figure 2. Comparison of the cutouts from the red filter of the DSS and the Sloan r filter of the GDS; angular size: approximately $100\times100''$.

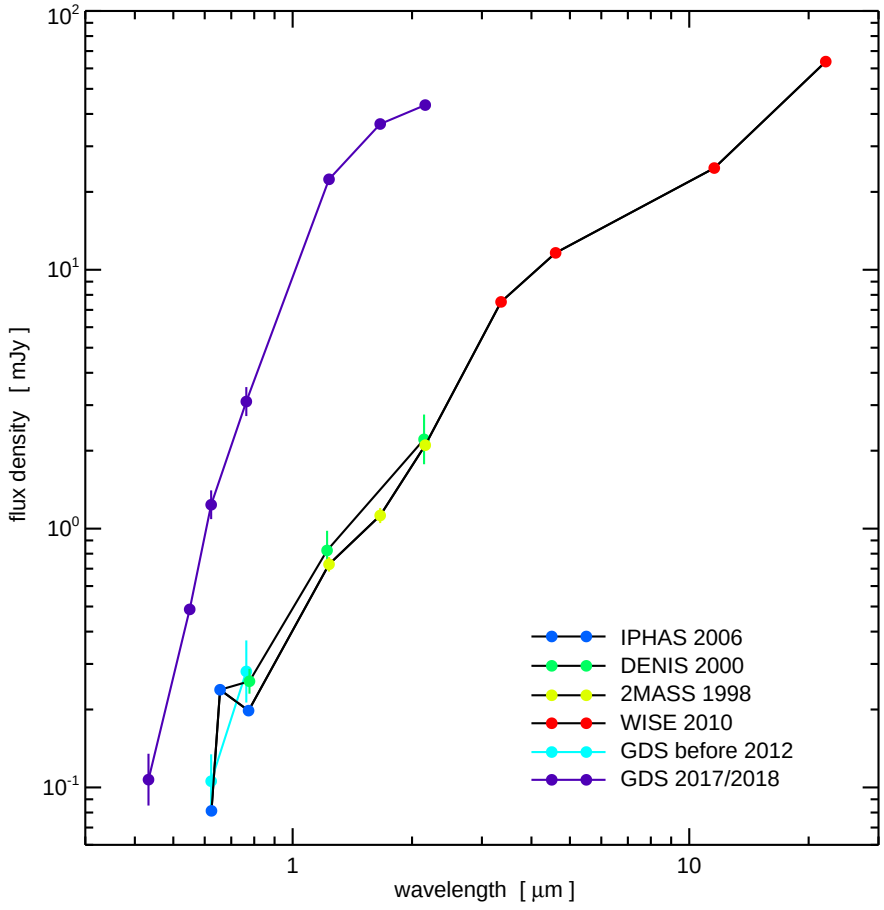

Figure 3. Spectral energy distribution; depicted GDS filters: B, V, r, i, J, H, K_s; error bars (if not seen) are smaller than the symbol size.

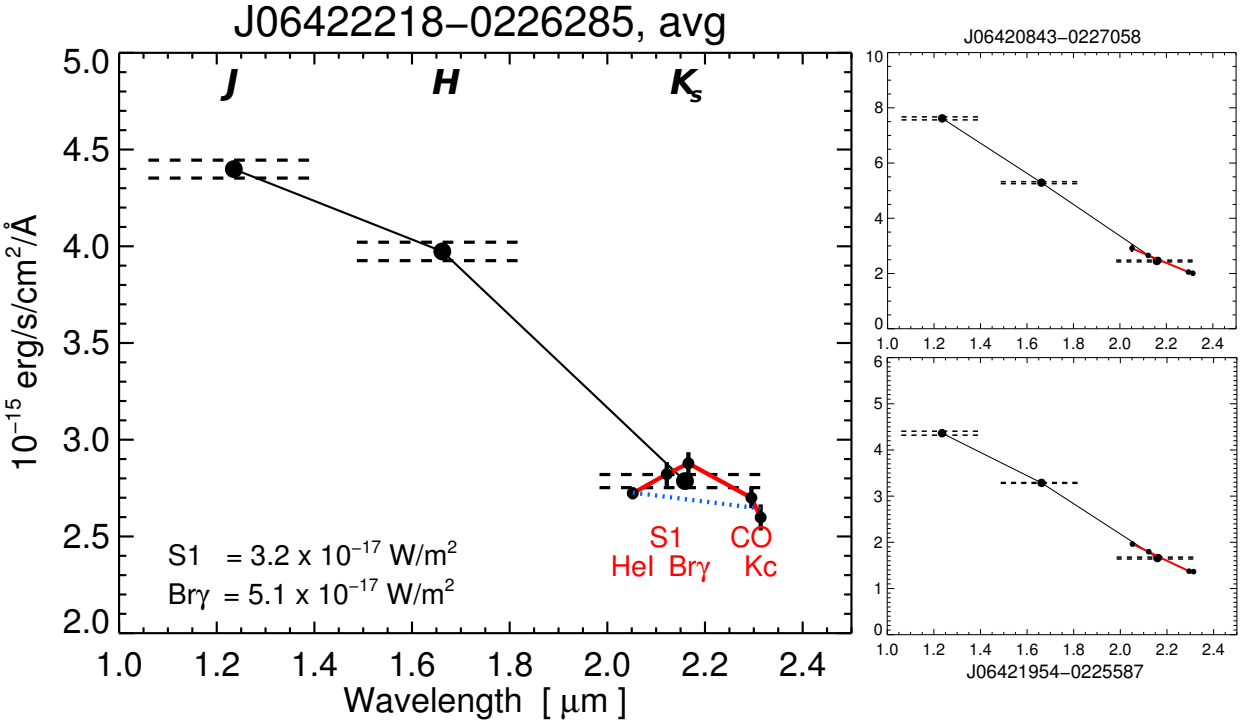

Figure 4. Average near infrared photometry of 2MASS J06422218–0226285 (left large panel) and two nearby stars of similar brightness (right, two small panels). The photometry was obtained in three nights in Feb–Mar 2018 with the IRIS telescope at USB in the broadband filters JHK_s and five narrow bands (FWHM = 275 Å) centered at 2.05, 2.121, 2.167, 2.29 and 2.314 μm (HeI, H_2 (1-0) S1, Brγ, CO, K_c, black filled circles connected with a red line). The horizontal dashed lines indicate the bandwidth and error range of the broadband J, H, K_s. For 2MASS J06422218-0226285 the error range in all bands is ∼2%, thus significantly larger than for other nearby stars of similar brightness (< 0.5%); this indicates a remaining small variability of 2MASS J06422218–0226285. For 2MASS J06422218–0226285 the flux in the Brγ filter lies above both the K_s broadband flux and the continuum as interpolated between HeI and CO and K_c (blue dotted line). While HeI and CO absorption cannot be ruled out yet, for an outbursting object it appears more likely that Br_γ and hydrogen S1 are in emission.

Table 1: Near-infrared photometry obtained in three nights in Feb–Mar. 2018 with IRIS.

Filter	λ	f_ν	f_ν error	flux	flux error
	μm	mJy	mJy	10^{-15} erg/s/cm^2/Å	10^{-15} erg/s/cm^2/Å
J	1.235	22.3641	0.235612	4.3988384	0.0463431
H	1.662	36.5833	0.438685	3.9732172	0.0476444
K_s	2.159	43.2917	0.527097	2.7862547	0.0339240
HeI	2.052	38.1709	0.437991	2.7232539	0.0312480
H_2 (1-0) S1	2.121	42.2975	0.928504	2.8223840	0.0619564
Brγ	2.166	44.9465	0.899277	2.8779934	0.0575820
CO	2.295	47.3339	0.944012	2.6997119	0.0538422
K_c	2.314	46.3109	1.20148	2.5981670	0.0674066

precisely measured stars with 2MASS quality flag A or B in all three filters. We searched a 1200″ box around the target to maintain a balance between the consideration of only the close environment of the star and sufficient statistics. This yields a rate of 1.49 % (16 out of 1077) K_s excess stars near J06422218–0226285. The resulting rate needs to be compared with the expected frequency of K_s excess stars near the galactic plane. For this purpose, we used the center coordinates of 15 randomly selected GDS fields with 6h < RA < 11h and investigated the 2MASS stars in a 1200″ box around these coordinates. In total, 26588 2MASS stars (with flag A, B) are covered by these boxes with 151 of them (0.57 %) being K-excess stars. To estimate the field-to-field fluctuation, the fraction of K-excess stars is calculated individually for each field and then averaged, resulting in a mean of 0.62 % and standard deviation of 0.31 %. Thus, the rate of K_s excess stars near J06422218–0226285 is almost 3σ above that of the mean. Note that only in one of the 15 boxes the rate of K-excess stars is as high as in the case of J06422218–0226285. Hence, one might speculate that J06422218–0226285 is located in a region of thin star formation or a star forming region at the end of its lifespan. Additionally, IRAS-IRIS and AKARI images indicate a nebulous surrounding. These findings, Hα emission before and Brγ emission after the outburst, and the present and past infrared excess support the claim of a YSO; albeit it is not close to a known star-forming region and there are no emission or reflection nebulae nor a high number of Hα objects near J06422218–0226285 and the amplitude is rather low for a FUor. Accordingly, these indications require further confirmation by spectroscopy.

Alternatively to a YSO, J06422218–0226285 could be a cataclysmic variable (CV). As already noted in Warner (1995a), some subclasses of CVs show stable high states after an outburst for several years up to decades (see, e.g., MV Lyr in Warner, 1995b, and RX And and TZ Per in Simonsen et al., 2014). It is believed that this is caused by a mass transfer feedback heating the secondary star. In this case, the Hα and Brγ emission can be explained by the surrounding accretion disk. Also, the irregular $r - i$ color variations of up to 0.8 mag fit this scenario.

Several features of J06422218–0226285 in the light curve and the SED are reminiscent of a symbiotic binary. Among them are the signs of circumstellar gas and dust and different variability effects on the time scales of days to months. These could explain the shape of the SED and the minor variations of the light curve after the outburst. Since the novae of symbiotic binaries rise up to 3 mag in the optical in a couple of years at most and last for up to a century (see Skopal, 2015 and Munari, 2012), the characteristics of the outburst of J06422218–0226285 fit this scenario as well.

Viironen et al. (2009) identified J06422218-0226285 as a planetary nebula candidate due to its position in IPHAS and 2MASS color-color diagrams. However, in a DENIS IJK_s color-color diagram (Fig. 5), the object lies outside of the area of PNs; instead it exhibits symbiotic Mira colors (see Schmeja & Kimeswenger, 2001 and Schmeja & Kimeswenger, 2003). Furthermore, the light curve does not fit a pulsating star, and the increase in brightness certainly is too vast and rapid for Post-AGB evolution. After the outburst, J06422218–0226285 still resides outside the area of PNs. Here, the I magnitude has been estimated from a black-body fit to the SED (Fig. 3).

To summarize, based on the Bochum Galactic Disk Survey, we detected a remarkable 3–4 mag outburst of J06422218–0226285 in 2013. The nature of the star is still puzzling. The multi-band photometry is consistent with a FUor- or EXor-type YSO, albeit the star is located in a thin star forming region. Also, the alternatives of a cataclysmic variable or a symbiotic binary or a PN/post-AGB are possible. In any case, the system shows

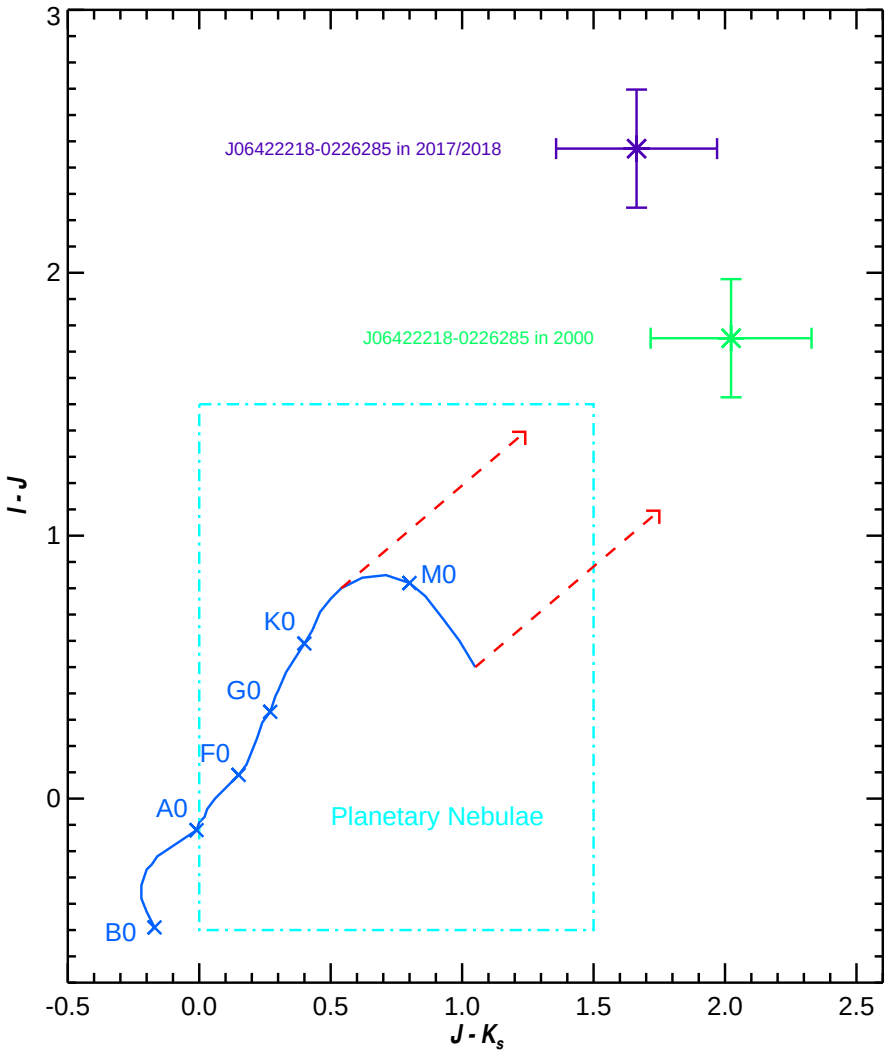

Figure 5. IJK_s color-color diagram: blue curve – main sequence stars; blue crosses – position of B0, A0, F0, G0, K0, M0 stars; red dashed-dotted lines – reddening paths for $A_V = 3.5$; cyan area – expected colors for planetary nebulae; green and purple cross – 2MASS J06422218–0226285.

exceptionally rare features, worth to clarify with future observations (e. g. spectroscopic or X-ray or radio).

Acknowledgements: We thank the referee for the instructive comments.

References:

Barentsen, G., Farnhill, H. J., Drew, J. E., et al., 2014, *MNRAS*, **444**, 3230 DOI
Blex, S., 2017, Variable Infrared Excess Objects from the Bochum Galactic Disk Survey, Master Thesis, Ruhr-Universität Bochum
Carr, J. S. & Tokunaga, A. T., 1992, *ApJL*, **393**, L67 DOI
Epchtein, N., de Batz, B., Copet, E., et al., 1994, *ApSS*, **217**, 3 DOI
Haas, M., Hackstein, M., Ramolla, M., Drass, H., Watermann, R., Lemke, R., & Chini, R., 2012, *AN*, **333**, 706 DOI
Hackstein, M., Fein, C., Haas, M., et al., 2015, *AN*, **336**, 590 DOI
Lasker, B. M., Lattanzi, M. G., McLean, B. J., et al., 2008, *AJ*, **136**, 735 DOI
Munari, U., 2012, *JAAVSO*, **40**, 572
Schmeja, S. & Kimeswenger, S., 2001, *A&A*, **377**, L18 DOI
Schmeja, S. & Kimeswenger, S., 2003, *ASPC Series*, **303**, 446
Simonsen, M., Boyd, D., Goff, W., et al., 2014, *JAAVSO*, **42**, 177
Skopal, A., 2015, *ASPC Series*, **496**, 226
Skrutskie, M. F., Cutri, R. M., Stiening, R., et al., 2006, *AJ*, **131**, 1163 DOI
Viironen, K., Mampaso, A., Corradi, R. L. M., et al., 2009, *A&A*, **502**, 113 DOI
Warner, B., 1995a, Cataclysmic Variable Stars, *Cambridge Astrophysics Series* 28, Cambridge University Press
Warner, B., 1995b, *ApSS*, **230**, 83 DOI
Wright, E. L., Eisenhardt, P. R. M., Mainzer, A. K., et al., 2010, *AJ*, **140**, 1868 DOI

Table 2: GDS r magnitudes; the first line gives the magnitude of co-added images between 2010 and 2012.

MJD	**mag**	**err**	**MJD**	**mag**	**err**	**MJD**	**mag**	**err**
55197-55927	18.840	0.260	56949.270	16.364	0.145	57791.030	16.306	0.140
56246.235	17.538	0.377	56953.250	16.338	0.142	57800.043	16.278	0.137
56377.999	17.347	0.324	56963.259	16.333	0.141	57804.022	16.151	0.124
56541.379	17.173	0.281	56964.242	16.375	0.146	57806.020	16.337	0.144
56547.376	16.997	0.244	56965.229	16.439	0.154	58008.386	16.230	0.132
56551.386	17.184	0.284	56966.229	16.414	0.151	58011.375	16.327	0.143
56558.372	17.176	0.282	56967.218	16.487	0.160	58012.381	15.992	0.108
56561.326	17.241	0.297	56968.217	16.063	0.113	58014.379	16.146	0.123
56571.313	16.958	0.236	56969.216	16.501	0.162	58015.372	16.175	0.126
56572.368	16.929	0.231	56978.220	16.349	0.143	58016.374	16.047	0.113
56576.293	17.529	0.374	56979.217	16.260	0.133	58018.364	16.195	0.128
56577.290	17.170	0.281	56980.215	16.214	0.128	58019.363	16.559	0.173
56586.329	16.629	0.180	56981.211	16.203	0.127	58021.356	16.350	0.146
56588.334	17.092	0.263	56982.209	16.363	0.145	58022.353	16.385	0.150
56591.360	16.809	0.209	56983.205	16.121	0.118	58023.350	16.176	0.126
56615.275	16.854	0.217	56984.202	16.324	0.140	58024.349	15.931	0.103
56616.287	16.473	0.159	57308.297	16.342	0.142	58025.345	16.132	0.122
56617.226	16.589	0.174	57311.297	15.980	0.105	58027.347	16.244	0.133
56619.207	16.703	0.192	57317.256	16.236	0.130	58028.337	16.270	0.136
56620.208	16.616	0.178	57318.256	16.134	0.120	58030.336	16.081	0.117
56622.199	16.484	0.160	57320.256	16.173	0.124	58032.327	16.298	0.140
56623.176	16.904	0.226	57321.256	16.232	0.130	58033.324	16.404	0.152
56624.176	16.785	0.205	57322.256	16.438	0.154	58034.322	16.297	0.140
56625.176	16.455	0.156	57323.256	16.334	0.141	58035.309	16.196	0.128
56626.177	16.571	0.172	57324.312	16.246	0.131	58036.316	16.283	0.138
56627.179	16.743	0.198	57325.299	16.154	0.122	58037.312	16.023	0.111
56641.126	16.565	0.171	57328.256	16.116	0.118	58038.314	16.365	0.148
56642.129	16.546	0.168	57330.266	16.071	0.114	58039.338	16.252	0.134
56646.116	16.308	0.138	57331.224	16.072	0.114	58040.298	16.188	0.127
56647.117	16.787	0.205	57332.224	16.248	0.132	58041.295	16.037	0.112
56648.119	16.544	0.168	57333.224	16.268	0.134	58042.292	16.231	0.132
56649.105	16.676	0.187	57334.224	16.325	0.140	58043.289	16.271	0.137
56653.106	16.653	0.184	57338.224	16.164	0.123	58044.331	16.037	0.112
56654.107	16.232	0.130	57655.340	15.934	0.101	58045.352	15.971	0.107
56660.305	16.313	0.139	57657.335	16.130	0.119	58046.341	16.155	0.124
56661.304	16.410	0.150	57658.336	16.147	0.121	58047.363	16.135	0.122
56665.267	16.146	0.121	57659.367	16.094	0.116	58049.310	16.166	0.125
56667.275	16.279	0.135	57660.322	15.997	0.107	58050.356	15.967	0.106
56668.266	16.322	0.140	57784.034	16.498	0.165	58051.342	16.032	0.112
56669.263	16.217	0.128	57785.034	16.201	0.129	58052.364	16.102	0.119
56937.286	16.458	0.157	57786.033	16.340	0.145	58053.359	16.141	0.123
56938.348	16.203	0.127	57787.033	16.351	0.146	58056.293	16.151	0.124
56941.291	16.275	0.135	57788.032	16.152	0.124	58057.350	16.212	0.130
56942.291	16.411	0.151	57789.032	16.051	0.114	58058.360	16.311	0.141
56943.285	16.298	0.137	57790.032	16.202	0.129	58097.696	16.170	0.139

Table 3: GDS i magnitudes; the first line gives the magnitude of co-added images between 2010 and 2012.

MJD	**mag**	**err**	**MJD**	**mag**	**err**
55197-55927	17.780	0.300	56967.218	15.441	0.167
56362.121	16.376	0.354	56968.217	15.369	0.157
56541.379	16.037	0.271	56969.216	15.187	0.135
56547.376	15.989	0.261	56978.220	15.198	0.136
56548.378	15.890	0.241	56979.217	15.217	0.138
56551.386	15.979	0.259	56980.215	15.262	0.143
56558.372	16.114	0.288	56981.211	15.244	0.141
56560.341	16.081	0.281	56982.209	15.085	0.124
56561.326	16.053	0.275	56983.205	15.005	0.116
56576.293	16.315	0.337	56984.202	15.256	0.143
56585.271	16.109	0.287	57308.297	15.164	0.132
56623.176	15.472	0.171	57311.297	15.109	0.126
56625.176	15.320	0.151	57317.256	15.175	0.133
56626.177	15.509	0.176	57318.256	15.132	0.129
56646.116	15.733	0.212	57320.256	15.232	0.140
56649.105	15.458	0.169	57321.256	15.244	0.141
56653.106	15.487	0.173	57322.256	15.285	0.146
56660.305	15.443	0.167	57323.256	15.212	0.138
56661.304	15.593	0.189	57324.312	15.311	0.150
56665.267	15.589	0.188	57325.299	15.296	0.148
56667.275	15.248	0.142	57328.256	15.126	0.128
56668.266	15.199	0.136	57330.266	15.428	0.165
56669.263	15.431	0.165	57331.224	15.229	0.140
56937.286	15.155	0.131	57332.224	15.228	0.140
56938.348	15.332	0.152	57333.224	15.303	0.149
56941.291	15.326	0.151	57334.224	15.253	0.142
56942.291	15.261	0.143	57338.224	15.190	0.135
56943.285	15.288	0.147	57655.340	14.994	0.115
56949.270	15.318	0.150	57657.335	15.046	0.120
56953.250	15.354	0.155	57658.336	15.127	0.128
56963.259	15.336	0.153	57659.367	15.058	0.121
56964.242	15.165	0.132	57660.322	15.172	0.133
56965.229	15.396	0.161	58097.696	15.173	0.140
56966.229	15.294	0.147			